

# Seeing the World through an Antenna's Eye: Reception Quality Visualization Using Incomplete Technical Signal Information

Leif Bergerhoff

German Aerospace Center (DLR)  
German Remote Sensing Data Center (DFD)  
National Ground Segment (NBS)  
Neustrelitz, Germany  
Leif.Bergerhoff@dlr.de

**Abstract**—We come up with a novel application for image analysis methods in the context of direction dependent signal characteristics. For this purpose, we describe an inpainting approach adding benefit to technical signal information which are typically only used for monitoring and control purposes in ground station operations. Recalling the theoretical properties of the employed inpainting technique and appropriate modeling allow us to demonstrate the usefulness of our approach for satellite data reception quality assessment. In our application, we show the advantages of inpainting products over raw data as well as the rich potential of the visualization of technical signal information.

**Index Terms**—signal information, satellite data reception, inpainting, homogeneous diffusion, partial differential equations, data analysis, modeling, application

## I. INTRODUCTION

A fundamental part of daily operations at a ground station is the surveillance and evaluation of the data exchange with satellites. This requires good knowledge of the status and health of all equipment and services which are part of the reception and transmission chains. Due to the tremendous system complexity, the resulting high dimensionality of the available raw information, and the large number of different satellite contacts, a reliable manual quality and error analysis is not feasible if impossible. As a real-time data center for remote sensing and small scientific satellites, the ground station Neustrelitz was involved in about 17 000 operational satellite contacts in more than 26 missions in 2023. This includes earth observation satellites like EnMAP [10], TerraSAR-X [11], and Landsat 9 [12] as well as DSCOVR [13] in a space weather context. Currently, operational communication with satellites results in about 19 GiB of device and signal specific measurements every year. These numbers underline the necessity of advanced signal analysis techniques for the processing of technical signal information in a real-world scenario. Additionally, the available data is often only available in parts and not for a complete domain which represents another challenge. Signal level information for antenna pointing directions serve as a good example here. They are not available

for the whole range of possible directions but only for those of past satellite orbits.

Within the image analysis community, so-called inpainting techniques are a common tool to complete missing information. The technique of homogeneous diffusion inpainting suits well to restore image data from edges [3]–[6] or based on selected data points [7]–[9]. Another application is the field of image compression [1]. In a recent publication [2], Peter et al. relate traditional homogeneous diffusion inpainting and neural networks.

### A. Our Contributions

We present a novel approach which links technical signal information from ground station operations with well established tools from image analysis. The presented method employs homogeneous diffusion inpainting to create a two-dimensional visualization of directional dependent measurements from incomplete data. In our application, we demonstrate the usefulness of our approach for reception quality assessment. As input data, we use signal level information from operational S-band [14] data reception as well as the corresponding antenna pointing directions. We visualize the inpainted result and show its potential for exploration and assessment of technical signal information. To the best of our knowledge, this is the first attempt to combine ground station metadata and inpainting techniques. We see our contribution as a starting point for a comprehensive analysis of the technical signal information gained in operations with the aim of ground station development.

### B. Structure of the Paper

In Section II, we give a brief introduction to the technical signal information which motivate the development of our method and serve as a data basis for our application. Section III contains the mathematical background of homogeneous diffusion inpainting for two-dimensional direction dependent data. Section IV presents a real-world application and gives results of inpainted signal level information for

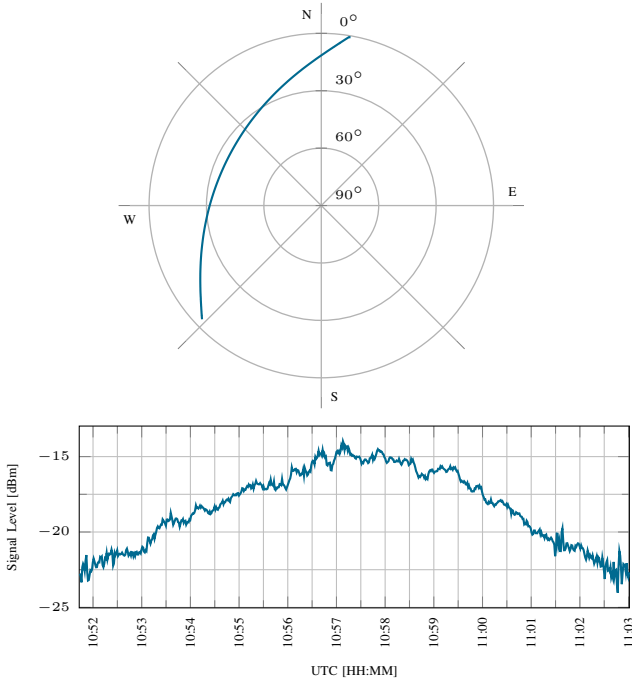


Fig. 1. An excerpt of technical signal information from a Landsat 9 satellite contact in September 2023. **Top:** Antenna pointing. **Bottom:** Measured Signal level.

antenna pointing directions. We conclude with a summary and outlook in Section V.

## II. TECHNICAL SIGNAL INFORMATION

Typically, communications with earth observation satellites at the ground station Neustrelitz last slightly more than 12 minutes. During this time, the related hardware and software provide status information about the currently received signal and the extracted data. This includes

- antenna systems (e.g. *antenna pointing information*),
- modems (e.g. *signal level information*), and
- front end processors (e.g. *extracted telemetry data information*).

Subsequently, we refer to this data as technical signal information. Usually, information is available as time-series data with a sampling interval of one second. I.e. a 12 minute satellite contact results in 720 measurements for each device involved in the communication process. In our case, one measurement can contain values for up to 80 parameters in parallel.

In Fig. 1, we provide an example for technical signal information which we store in our database. On top, one can see the antenna pointing in terms of the elevation  $\theta$  (0 to 90 degrees) and azimuth  $\varphi$  (0 to 360 degrees) angle. The corresponding signal level over time is illustrated below. The signal levels are given in decibel-milliwatts (dBm), i.e. given a power  $P$  in milliwatts (mW), the corresponding power level  $x$  in dBm is given by:

$$x = 10 \cdot \log_{10} \frac{P}{1 \text{ mW}}. \quad (1)$$

Usually, technical signal information serve for monitoring and control purposes of the ground station during satellite data reception and transmission. Subsequently, we show their additional benefit for reception quality assessment.

## III. MODELING / THEORY

### A. Problem Description

Let  $\mathbf{x} = (\theta, \varphi)^\top$  denote an antenna pointing direction, whereas  $\theta \in [0, \pi/2]$  represents the elevation angle and  $\varphi \in [0, 2\pi]$  represents the azimuth angle. Based on this, we define the two-dimensional domain spanned by azimuth and elevation as

$$\Omega := \{\mathbf{x} \mid \forall \theta \in [0, \frac{\pi}{2}], \varphi \in [0, 2\pi]\}. \quad (2)$$

For the set  $\Omega_K \subset \Omega$  of known data, we have signal level information

$$f(\mathbf{x}) : \Omega_K \rightarrow \mathbb{R}, \quad (3)$$

available.  $\Omega_K$  is also called *inpainting data*. Our aim is to fill in the missing signal level information in the so-called *inpainting domain*  $\Omega \setminus \Omega_K$  based on  $f$ . This process of filling in is called *inpainting*.

### B. Homogeneous Diffusion Inpainting

To estimate the missing data, we make use of a well-known and elegant technique called homogeneous diffusion inpainting. Within this context, we describe the desired signal level at time  $t$  as  $u := u(\mathbf{x}, t)$  with

$$u(\mathbf{x}, t) : \Omega \times [0, \infty) \rightarrow \mathbb{R}. \quad (4)$$

The time  $t$  serves as a model parameter and we focus on the scenario  $t \rightarrow \infty$ . Using the known data  $f$  as Dirichlet boundary conditions, we estimate  $u$  by solving the Laplace equation on the set of *unknown* data  $\Omega \setminus \Omega_K$ :

$$u(\mathbf{x}) = f(\mathbf{x}) \quad \text{for } \mathbf{x} \in \Omega_K, \quad (5)$$

$$\Delta u(\mathbf{x}) = 0 \quad \text{for } \mathbf{x} \in \Omega \setminus \Omega_K, \quad (6)$$

Referring to the real-world antenna pointing directions, we make use of mixed boundary conditions that model the periodicity of the azimuth domain and the point symmetry w.r.t. the point  $(\pi/2, \varphi)$ . Furthermore, we take into account homogeneous Neumann boundary conditions for  $\theta = 0$ . Consequently, we have:

$$\partial_\theta u|_{\theta=0} = 0, \quad (7)$$

$$u(\frac{\pi}{2} + \Delta\theta, \varphi, t) = u(\frac{\pi}{2} - \Delta\theta, \varphi + \pi, t), \quad (8)$$

$$u(\theta, 2\pi, t) = u(\theta, 0, t) \quad \forall \theta \in [0, \frac{\pi}{2}]. \quad (9)$$

Keeping this in mind, we can write our inpainting problem as

$$c(\mathbf{x})(u(\mathbf{x}) - f(\mathbf{x})) - (1 - c(\mathbf{x}))\Delta u(\mathbf{x}) = 0. \quad (10)$$

The confidence function  $c(\mathbf{x})$  – also referred to as *inpainting mask* – indicates whether a point is known or not:

$$c(\mathbf{x}) = \begin{cases} 1 & \text{for } \mathbf{x} \in \Omega_K, \\ 0 & \text{for } \mathbf{x} \in \Omega \setminus \Omega_K. \end{cases} \quad (11)$$

TABLE I  
A MINIMAL EXAMPLE ILLUSTRATING THE BOUNDARY CONDITIONS IN  
OUR DISCRETE SETUP.

	$u_{4,2}$	$u_{4,3}$	$u_{4,0}$	$u_{4,1}$	
$u_{4,3}$	$u_{4,0}$	$u_{4,1}$	$u_{4,2}$	$u_{4,3}$	$u_{4,0}$
$u_{3,3}$	$u_{3,0}$	$u_{3,1}$	$u_{3,2}$	$u_{3,3}$	$u_{3,0}$
$u_{2,3}$	$u_{2,0}$	$u_{2,1}$	$u_{2,2}$	$u_{2,3}$	$u_{2,0}$
$u_{1,3}$	$u_{1,0}$	$u_{1,1}$	$u_{1,2}$	$u_{1,3}$	$u_{1,0}$
$u_{0,3}$	$u_{0,0}$	$u_{0,1}$	$u_{0,2}$	$u_{0,3}$	$u_{0,0}$
	$u_{0,0}$	$u_{0,1}$	$u_{0,2}$	$u_{0,3}$	

The Laplacian of  $u$  is given by

$$\Delta u = \partial_{\theta\theta} u + \partial_{\varphi\varphi} u. \quad (12)$$

### C. Discrete Theory

Our goal is to solve the inpainting problem on the discrete elevation-azimuth domain which we assume to be a regular two-dimensional grid. In total, we make use of  $N$  different pointing directions, i.e.  $(\theta, \varphi)_i$  for  $i \in \{1, \dots, N\}$ . Storing the two-dimensional information row-wise, we represent the discrete version of the known data  $f$  as a one-dimensional vector  $\mathbf{f}$  and the desired signal  $u$  by means of the one-dimensional vector  $\mathbf{u}$ . Furthermore, we denote the  $i$ -th element in  $\theta$  and the  $j$ -th element in  $\varphi$  direction by  $f_{i,j}$  and  $u_{i,j}$ . Using a binary pixel mask  $c$  as the discrete counterpart of (11), we express whether signal information is known or not, i.e.  $c_i = 0$  for unknown pixels and  $c_i = 1$  for known pixels. Consequently, the discrete version of (10) reads

$$\mathbf{C}(\mathbf{u} - \mathbf{f}) - (\mathbf{I} - \mathbf{C})\mathbf{A}\mathbf{u} = 0, \quad (13)$$

where  $\mathbf{I}$  is the identity matrix and  $\mathbf{C} := \text{diag}(c)$  is a diagonal matrix containing the elements of  $c$  on its diagonal. Considering the boundary conditions (7)–(9), the symmetric  $N \times N$  matrix  $\mathbf{A}$  implements the discrete Laplace operator  $\Delta_{i,j}$  by means of central finite differences and the grid sizes  $h_\theta$  and  $h_\varphi$ , where

$$\partial_{\theta\theta} u_{i,j} \approx \frac{u_{i+1,j} - 2u_{i,j} + u_{i-1,j}}{h_\theta^2}, \quad (14)$$

$$\partial_{\varphi\varphi} u_{i,j} \approx \frac{u_{i,j+1} - 2u_{i,j} + u_{i,j-1}}{h_\varphi^2}. \quad (15)$$

A minimal example which illustrates the boundary conditions for  $\mathbf{u}$  can be found in Table I.

From (13) one can derive the linear systems of equations

$$\underbrace{(\mathbf{C} - (\mathbf{I} - \mathbf{C})\mathbf{A})}_{:=\mathbf{M}} \mathbf{u} = \mathbf{C}\mathbf{f}. \quad (16)$$

This system of equations has a unique solution which fulfills a maximum-minimum principle. To prove this, we borrow the proof from [1], chapter 2.4, which directly applies to our problem. Its basic idea is to show positive definiteness of  $\mathbf{M}$  using Gershgorin's circle theorem [16] in combination with the block irreducibility property discussed in [15].

## IV. APPLICATION

Next, we want to combine antenna pointing information and microwave frequency feedback in order to visualize the reception quality of an S-band antenna for one year. In our case, we focus on the signal information related to the reception of the DSCOVER satellite. This comes down to a dataset containing  $\sim 14.95$  million measurements.

We make use of a digital image plane – which corresponds to the azimuth-elevation plane – with a fixed resolution, e.g.  $3600 \times 901$  px when using a precision of one for angles. At every position  $(\varphi, \theta)_i$ , we fill in the corresponding observed signal level. Whenever overlaps of the input data – due to resolution restrictions – occur in the image plane, we average the input data. Please note, that in all subsequent illustrations of signal level information, we apply an affine greyscale transformation for better visualization.

In Fig. 2, we show the signal level w.r.t. antenna pointing directions. The x-direction corresponds to the azimuth angles  $\varphi$ , the y-direction to elevation angles  $\theta$  (with  $\theta = 0^\circ$  at the bottom and  $\theta = 90^\circ$  at the top). Black areas indicate missing information. On the top, one can see the satellite trajectories from the antenna's point of view combined with signal level information. The higher the signal level, the brighter the pixel. There is one trajectory for every day of the year. Since the DSCOVER satellite is positioned at the Sun-Earth  $L_1$  Lagrange point, the trajectories roughly correspond to the position of the sun. I.e. the trajectories with largest average elevation  $\theta$  are close to summer solstice (azimuth angles between 56 and 304 degrees). On the other hand, the lowest trajectories – in terms of small average elevation  $\theta$  – are close to winter solstice (azimuth angles between 139 and 221 degrees).

In the bottom image of Fig.2, we illustrate the result of homogeneous diffusion inpainting. The inpainting keeps the known data untouched (inpainting mask set to one) and completes missing signal level information in the remaining areas. Aside a trajectory with low signal level in the afternoon (the dark arc section on the right side of the illustration), the inpainted result emphasizes structures which can hardly be recognized in the raw data. This includes data at the bottom of the picture (which correspond to the ground), as well as features in the sky.

This becomes especially clear by taking a closer look at Fig. 3. This excerpt of the inpainted signal level information from the morning hours and close to the ground contains significant shadows. By taking a look at the corresponding camera picture, one can see that these shadows correspond to buildings and antenna systems of the ground station. Even the trees on the right hand side are visible in the signal level information.

Another example from the evening hours of satellite data reception close to the ground is given in Fig. 4. Therein, we see that the signal quality gets degraded due to an antenna system impairing the signal line of sight.

Apart from buildings, antenna systems, and natural obstacles, the inpainted signal information highlights further drops

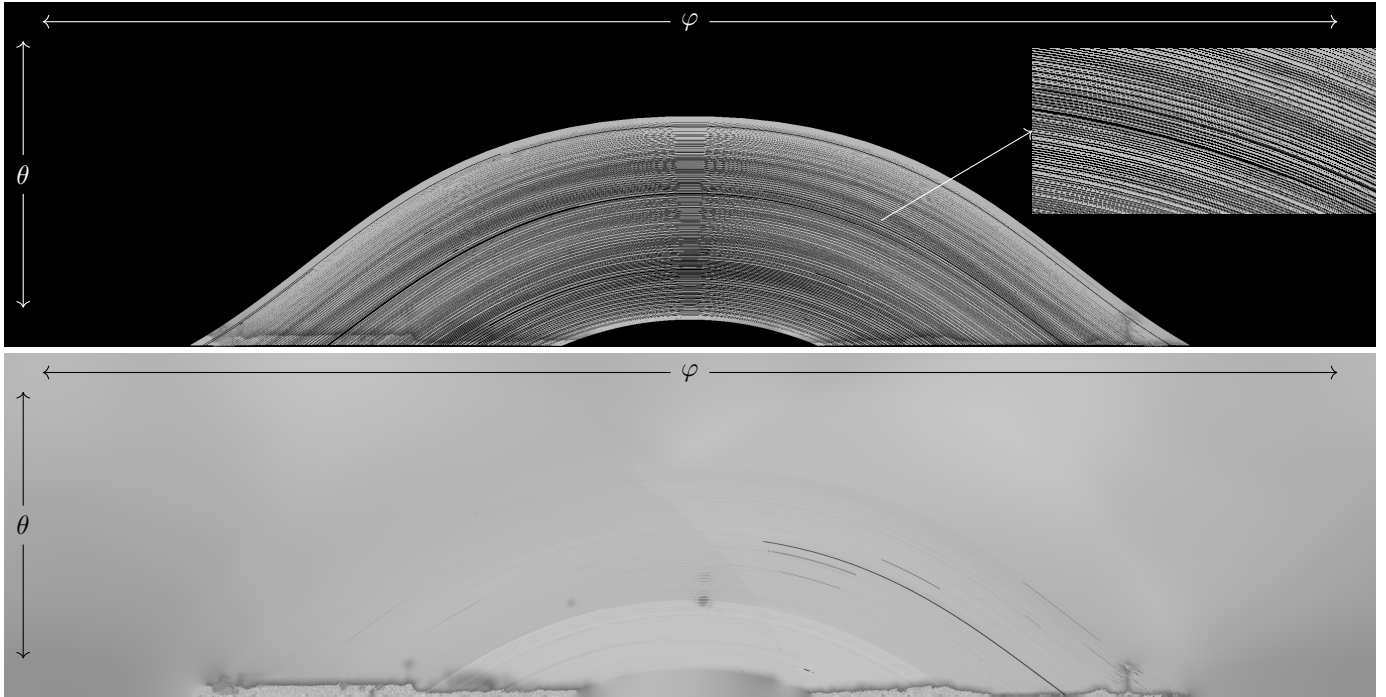


Fig. 2. **Top:** Image ( $3600 \times 901$  pixels) showing trajectories of the DSCOVR satellite and the corresponding signal level information from the antenna's reception perspective. **Bottom:** Result of homogeneous diffusion inpainting after 6412 iterations using  $\varepsilon = 10^{-8}$ .

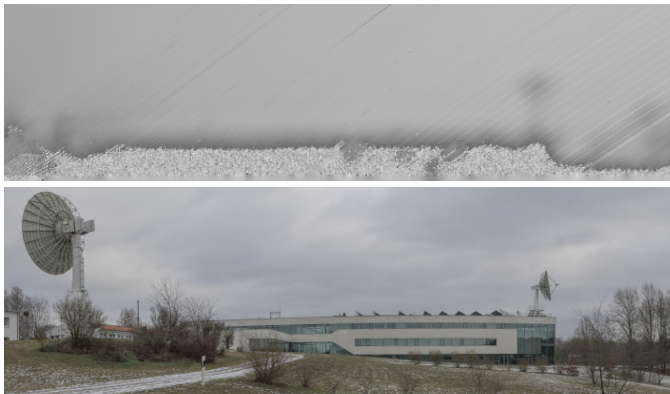


Fig. 3. **Top:** Enlarged section of the inpainted signal level information for small elevation  $\theta$  in the morning hours. **Bottom:** Corresponding camera picture of the ground station from the antenna's point of view.



Fig. 4. **Top:** Section of the inpainted signal level information for small elevation  $\theta$  in the evening. **Bottom:** Camera picture of the corresponding region from the antenna's point of view.

in the signal level around noon and in the late morning hours (see Fig. 5, top). Now, recall that this visualization offers a summary view over one year of data reception. This means that the degradation of the signal level occurred for almost identical antenna pointing angles for a number of subsequent days. With the help of our visualization, we are also able to detect these – in raw data – easily overlooked events. However, the reasons for this degradations are still under investigation by the ground station development team.

Apart from that, one can recognize a conspicuous pattern – similar to a staircase – at noon time throughout all trajectories where the signal level increases from left to right (see Fig. 2).

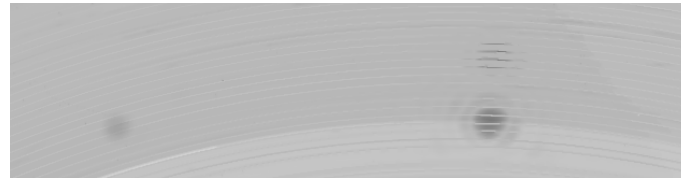


Fig. 5. Highlighted drops in the signal level for an as yet unknown reason.

This effect correlates with a change in the satellite's data transmission rate which increases every day in this time period.

## A. Implementation Details and Runtime

We solve the linear system of equations (16) using the method of conjugate gradients [17]. As a stopping criterion, we employ a threshold of  $\varepsilon$  on the relative residual decay in the  $L^2$ -norm. We came up with an implementation in C which pays special attention to the sparseness of the matrix  $M$ . Consequently, the space and time complexity per iteration of the algorithm is  $\mathcal{O}(m)$ , where  $m$  denotes the number of nonzero entries of  $M$ . The computation time for the result shown in Fig. 2 was about 62 seconds using 20 threads of a Intel i7-12800H Processor.

## V. SUMMARY AND OUTLOOK

Our paper shows the high potential of inpainting techniques for technical signal information, especially, in the context of satellite data reception. The visualization of the gained quality information product allows the identification and treatment of potential problems within our satellite data reception chain which might be overseen otherwise.

In our future work, we will take a look at the solution of the inpainting problem in different coordinate systems. In terms of antenna pointing directions, spherical coordinates might be a more appropriate approach. This, however, comes at the cost of a more comprehensive well-posedness analysis regarding the underlying mathematical problem.

Furthermore, we also plan to expand our inpainting approach to support input data from additional sources like digital images. A sensor fusion strategy is highly likely to cope better with missing information. Connected to this idea is the consideration of anisotropic inpainting methods. In this way, existing structures within the input data could be better reflected in the result.

Our contribution has already proven to be a valuable tool for the evaluation of satellite data reception and the development of the ground station Neustrelitz.

## ACKNOWLEDGMENT

I thank my colleagues at DLR, especially Robert Miesen and Jens Richter for valuable comments and fruitful discussions. The latter has also provided the photos being used in this paper.

## REFERENCES

- [1] M. Mainberger, "Pde-based image compression based on edges and optimal data," Ph.D. dissertation, Saarland University, 2015.
- [2] P. Peter, K. Schrader, T. Alt, and J. Weickert, "Deep spatial and tonal data optimisation for homogeneous diffusion inpainting," *Pattern Analysis and Applications*, vol. 26, no. 4, pp. 1585–1600, 2023.
- [3] S. Carlsson, "Sketch based coding of grey level images," *Signal processing*, vol. 15, no. 1, pp. 57–83, 1988.
- [4] J. H. Elder, "Are edges incomplete?" *International Journal of Computer Vision*, vol. 34, no. 2-3, pp. 97–122, 1999.
- [5] R. Hummel and R. Moniot, "Reconstructions from zero crossings in scale space," *IEEE Transactions on Acoustics, Speech, and Signal Processing*, vol. 37, no. 12, pp. 2111–2130, 1989.
- [6] D. Rotem and Y. Y. Zeevi, "Image reconstruction from zero crossings," *IEEE Trans. Acoust. Speech Signal Process.*, vol. 34, no. 5, pp. 1269–1277, 1986.
- [7] P. Johansen, S. Skelboe, K. Grue, and J. D. Andersen, "Representing signals by their toppoints in scale space," in *Proceedings of the 8th International Conference on Pattern Recognition (Paris, France, October 1986)*, 1986, pp. 215–217.
- [8] F. Kanters, M. Lillholm, R. Duits, B. J. Janssen, B. Platel, L. Florack, and B. M. ter Haar Romeny, "On image reconstruction from multiscale top points," in *Scale Space and PDE Methods in Computer Vision, 5th International Conference, Scale-Space 2005, Hofgeismar, Germany, April 7-9, 2005, Proceedings*, ser. Lecture Notes in Computer Science, R. Kimmel, N. A. Sochen, and J. Weickert, Eds., vol. 3459. Springer, 2005, pp. 431–442.
- [9] M. Lillholm, M. Nielsen, and L. D. Griffin, "Feature-based image analysis," *International Journal of Computer Vision*, vol. 52, no. 2-3, pp. 73–95, 2003.
- [10] T. Storch, H.-P. Honold, S. Chabrilat, M. Habermeyer, P. Tucker, M. Brell, A. Ohndorf, K. Wirth, M. Betz, M. Kuchler, H. Mühle, E. Carmona, S. Baur, M. Mücke, S. Löw, D. Schulze, S. Zimmermann, C. Lenzen, S. Wiesner, S. Aida, R. Kahle, P. Willburger, S. Hartung, D. Dietrich, N. Plesia, M. Tegler, K. Schork, K. Alonso, D. Marshall, B. Gerasch, P. Schwind, M. Pato, M. Schneider, R. de los Reyes, M. Langheinrich, J. Wenzel, M. Bachmann, S. Holzwarth, N. Pinnel, L. Guanter, K. Segl, D. Scheffler, S. Foerster, N. Bohn, A. Bracher, M. A. Soppa, F. Gascon, R. Green, R. Kokaly, J. Moreno, C. Ong, M. Sornig, R. Wernitz, K. Bagschik, D. Reintsema, L. La Porta, A. Schickling, and S. Fischer, "The enmap imaging spectroscopy mission towards operations," *Remote Sensing of Environment*, vol. 294, p. 113632, Aug. 2023.
- [11] B. Schättler, F. Mrowka, E. Schwarz, and M. Lachaise, "The TerraSAR-X ground segment in service for nine years: Current status and recent extensions," in *2016 IEEE International Geoscience and Remote Sensing Symposium*. IEEE, Jul. 2016, pp. 1400–1403.
- [12] B. Markham, J. Barsi, E. Donley, B. Efremova, J. Hair, D. Jenstrom, E. Kaita, E. Knight, G. Kvaran, J. McCorkel, M. Montanaro, E. Morland, A. Pearlman, J. Pedelty, and B. Wenny, "Landsat 9: Mission status and prelaunch instrument performance characterization and calibration," in *IGARSS 2019 - 2019 IEEE International Geoscience and Remote Sensing Symposium*. IEEE, Aug. 2019, pp. 5788–5791.
- [13] J. Burt and B. Smith, "Deep space climate observatory: The DSCOVR mission," in *2012 IEEE Aerospace Conference*. IEEE, Apr. 2012, pp. 1–13.
- [14] "IEEE standard letter designations for radar-frequency bands," *IEEE Std 521-2019 (Revision of IEEE Std 521-2002)*, pp. 1–15, 2020.
- [15] D. G. Feingold and R. S. Varga, "Block diagonally dominant matrices and generalizations of the gerschgorin circle theorem," *Pacific Journal of Mathematics*, vol. 12, no. 4, pp. 1241–1250, 1962.
- [16] S. Gerschgorin, "über die abgrenzung der eigenwerte einer matrix," *Bulletin de l'Académie des Sciences de l'URSS. Classe des sciences mathématiques et na*, no. 6, pp. 749–754, 1931.
- [17] M. R. Hestenes and E. Stiefel, "Methods of conjugate gradients for solving linear systems," *Journal of research of the National Bureau of Standards*, vol. 49, no. 6, pp. 409–436, Jul. 1952.